

A method to quantitatively assess the modes-of-action of flame-retardants

Mathieu Vangrevelynghe, Lucie Le Nouvel, Cécile Pesenti, Rodolphe Sonnier, Laurent Ferry, Emmanuelle Gesta, Christian Lagrève

▶ **To cite this version:**

Mathieu Vangrevelynghe, Lucie Le Nouvel, Cécile Pesenti, Rodolphe Sonnier, Laurent Ferry, et al.. A method to quantitatively assess the modes-of-action of flame-retardants. Polymer Degradation and Stability, 2022, 195, pp.109767. 10.1016/j.polymdegradstab.2021.109767 . hal-03412974

HAL Id: hal-03412974

https://imt-mines-ales.hal.science/hal-03412974

Submitted on 1 Jun 2022

HAL is a multi-disciplinary open access archive for the deposit and dissemination of scientific research documents, whether they are published or not. The documents may come from teaching and research institutions in France or abroad, or from public or private research centers.

L'archive ouverte pluridisciplinaire **HAL**, est destinée au dépôt et à la diffusion de documents scientifiques de niveau recherche, publiés ou non, émanant des établissements d'enseignement et de recherche français ou étrangers, des laboratoires publics ou privés.

A method to quantitatively assess the modes-of-action of flame-retardants

Mathieu Vangrevelynghe[a], Lucie Le Nouvel[a], Cécile Pesenti[a], Rodolphe Sonnier[a,*], Laurent Ferry[a], Emmanuelle Gesta[b], Christian Lagrève[b]

[a] *Polymers Composites and Hybrids (PCH), IMT Mines Ales, Ales, France*
[b] *ACOME, Centre de Romagny-Fontenay, Romagny-Fontenay, France*

A B S T R A C T

The assessment of the modes of action of flame retardants (FRs) and their quantification is a challenging issue. This study highlights that the condensed phase efficiency θ can be assessed by combining different flammability tests (pyrolysis-combustion flow calorimeter PCFC, Limiting Oxygen Index LOI, cone calorimeter). Relations were proposed to calculate LOI and pHRR in cone calorimeter from several parameters including θ. A satisfying agreement between experimental values and calculated ones were found for a set of several dozens of FR-free polymers assuming that $\theta = 1$ (i.e. no action in condensed phase).Then, θ was evaluated for EVA/PE blends containing Aluminium TriHydroxyde (ATH) and/or Magnesium DiHydroxyde (MDH) and for ABS containing Ammonium PolyPhosphate (APP) and/or DecaBromoDiPhenylOxide (DBDPO) assuming that LOI and pHRR of flame-retardant compositions follow the same relationships as those of unfilled polymers. The evolution of θ (as well as χ, i.e. the combustion efficiency) highlights the modes of action of FRs and can contribute to the discussion about possible synergy or antagonism between FRs. Especially, an apparent synergism between APP/DBDPO is observed in cone calorimeter from a performance point of view. Nevertheless, the calculation of χ and θ challenges this conclusion.

Keywords:
Polymer
Flame retardant
LOI
Cone calorimeter
Pyrolysis-combustion flow calorimetry
Synergy
FR mode-of-action

1. Introduction

Polymers are easily flammable, forcing to add flame-retardants to formulations. Many flame retardant systems improve the flame retardancy through different modes-of-action [1] in condensed phase (through char promotion or endothermic decomposition), or in gas phase (through radical trapping or dilution of fuels). Synergism between FRs is also often desired to improve the fire performances. For example, Ethylene Vinyl Acetate compounds are commonly used in the wire and cable industry, due to their outstanding properties (flexibility and elongation at break). EVA is flame retarded with high amount of fillers (up to 65%), especially with aluminium and/or magnesium hydroxide (ATH & MDH) [2,3]. In order to improve the fire retardancy of EVA compounds, many fillers were used in combination with ATH or MDH like nanofillers such as montmorillonite [4–7], or phosphorous based additives [8]. Other well-established synergistic systems can be cited, like halogen-antimony synergy [9] which has an effect in both condensed and gas phases thanks to Sb_2O_3 reaction with hydrogen halides. Ternary intumescent systems are another synergistic systems which promote the formation of a charred layer by a combined reaction between an acid source, a char forming agent and a blowing agent [10,11].

Assessing the relative efficiency of each mode-of-action would be useful to design better FR systems and to identify synergism between FRs. While actions in gas phase can be estimated through the measurement of the combustion efficiency χ, the efficiency of the action in condensed phase, i.e. the relative efficiency of heat and mass transfer at the solid surface (often called θ) cannot be easily evaluated. Moreover, the importance of modes-of-action depends on the fire scenario (i.e. on the flame test). Therefore, the efficiency of a FR may be significantly different from one test to another because test conditions and pass/fail criteria greatly differ. In LOI, the main criterion governing rating is the flame extinction after removal of the ignition source. In cone calorimeter, the burning is forced by exposing the material to a radiative source during the whole test.

As an example, Cogen et al. [12] compared performances of halogen-free flame retardants in EVA/PE blends for wire and cable industry using different tests. They found some correlations between PCFC and cone calorimeter, but no correlation was no-

* Corresponding author.
E-mail address: rodolphe.sonnier@mines-ales.fr (R. Sonnier).

ticed between LOI and PCFC. Schartel et al. [13] studied seventeen PC/ABS blends retarded with various additives. They found correlation between total heat release (THR) and char residue with the limiting oxygen index (LOI). But they showed a poor correlation with the heat release capacity (HRC or sumHRC) with a high dispersion of LOI from 15 to 45 for HRC close to 400 J/g.K.

This lack of correlation may be also used to assess the modes-of-action of FRs. Sonnier et al. [14] have evaluated the barrier effect of different fillers combining two methods (namely PCFC and cone calorimeter), based on the fact that some effects like flame inhibition or barrier effect cannot be observed in PCFC [15] but are efficient in cone calorimeter.

Different studies proposed equations to calculate LOI using various parameters. For example, Van Krevelen [16] proposed a relation between oxygen index and char yield measured in thermogravimetry (anaerobic pyrolysis). Lyon et al. [17, 18] suggested an equation where LOI is predicted from flammability parameters measured by PCFC [19]. Nevertheless, these approaches are suitable to a limited range of polymers and/or lead to meaningless values for some materials. More recently, Lyon et al. [18] develop a Fire Growth Capacity (FGC) from PCFC data. This index involves the specific heat of complete combustion and the temperatures at 5% and 95% conversion of solid to gaseous fuel, that can be assimilated respectively to the ignition temperature and the burning temperature at macroscale. FGC was correlated ($R^2 = 0,7$) with LOI for a wide range of polymers. Other equations have also been proposed to calculate the pHRR in cone calorimeter from parameters measured at microscale [17].

Moreover, a better quantification of FR modes-of-action is needed to assess properly synergism. Indeed, synergism is often claimed but rarely proved. Synergism [20] can be postulated based on performances only or by establishing specific mechanisms. Camino et al. [21] focused on the cyclic chemical process that controls the polymer combustion, and showed that the maximum synergistic effect should be obtained considering a quantitative ratio of the condensed to gas phase action.

Lewin [22] and Holdsworth [23] have defined several parameters to evaluate the synergy according to the results obtained in LOI.

This study principally focuses on two approaches proposed to assess the actions of different FR systems in two different fire tests (Limiting Oxygen Index and Cone calorimeter) using flammability data from Pyrolysis-Combustion Flow Calorimetry (PCFC). The goal of the study is to characterize quantitatively the efficiency in condensed phase of FRs, with the aim of clarifying the means of quantitatively evaluating the synergy between FRs. Several examples based on EVA/PE and ABS compounds are discussed. Different modes of action are studied using a halogen FR (DBDPO) which acts in the gas phase action and a phosphorus based compound (APP) which acts in condensed phase in order to evaluate if synergistic effects were obtained [1].

2. Experimental part

2.1. Description of the method

The determination of the limiting oxygen index involves the sustained ignition and the downward propagation of a flame along a vertically orientated sample. Therefore, LOI should be related to the laws which govern these two phenomena and particularly the flame propagation. Quintiere proposed a simplified theory for flame spread rate based on the hypothesis that spread is due to the ignition of a small volume heated by the flame. For thermally thin solids, which can be considered as a reasonable assumption for LOI specimen, the flame spread velocity V_f can thus be described by Eq. (1) [24]:

$$V_f = \frac{\dot{q}''_f \, \delta_f}{e \, \rho C_p \left(T_{ig} - T_0\right)} \tag{1}$$

With $\dot{q}''_f$ the heat flux from the flame, δ_f the length heated by the flame, e the sample thickness, ρ the sample density,C_p the heat capacity, T_{ig} the ignition temperature, T_0 the ambient temperature. In Eq. (1), V_f is supposed to be the flame velocity in free atmosphere, i.e. the oxygen concentration being 21 vol%. Additionally, V_f is affected by the variation of oxygen concentration X_{O2}. Nasr et al. in their work on confined fire showed that the heat flux from the flame $\dot{q}''_f$ is composed of a convective part which is proportional to X_{O2} and of a radiative part which is proportional to X_{O2}^4 [25]. In the case of LOI with downward flame spread, the radiative part of $\dot{q}''_f$ should be preponderant. Hence, the flame spread velocity should vary as:

$$V_f = k X_{O2}^4 \tag{2}$$

LOI can be considered as the value of oxygen concentration for which the flame spread velocity reaches a critical value V_{fc}, this value being independent of oxygen concentration. From these considerations, it can be proposed that:

$$LOI = X_{O2}^{free\,atm} \left(\frac{V_{fc}}{V_f^{free\,at}} \right)^{\frac{1}{4}} = 21 \times \left(\frac{V_{fc}}{\frac{\dot{q}''_f \, \delta_f}{e \, \rho C_p \left(T_{ig} - T_0\right)}} \right)^{\frac{1}{4}} \tag{3}$$

In the present method, it is proposed that some parameters of Eq. (3) are directly related to parameters measured in PCFC experiments. Thus, T_{ig} can be related to T_{max} the temperature at maximum pyrolysis rate in PCFC. Moreover, the heat flux from the flame $\dot{q}''_f$ can be written as:

$$\dot{q}''_f = \alpha \times HRC \times \chi \times \theta_{LOI} \tag{4}$$

With α an *ad hoc* parameter ($g.K.s^{-1}.m^{-2}$), HRC the heat release capacity ($J.g^{-1}.K^{-1}$) measured in PCFC and assessing the decomposition rate and the dilution of the polymer in condensed phase, χ the combustion efficiency assessing the gas phase action and θ the relative efficiency of FR in condensed phase (barrier effect or endothermic effect, and more generally all phenomena which are not effective in PCFC, i.e. which do affect neither HRC nor T_{max}).

The combustion efficiency χ was calculated as follows using PCFC and cone calorimeter parameters:

$$\chi = \frac{EHC_{cone}}{HCC_{PCFC}} \tag{5}$$

with

$$EHC = \frac{THR}{1 - f_{cone\ residue}} \; and \; HCC = \frac{THR}{1 - f_{PCFC\ residue}} \tag{6}$$

$f_{residue}$ is the mass fraction of residue and THR is the total heat release. χ was calculated by dividing the effective heat of combustion (EHC) of fuel gases in the cone calorimeter test by HCC, Heat of complete combustion, measured at PCFC [26,27]. χ characterizes especially the flame inhibition. It cannot be calculated using PCFC in standard conditions because combustion is assumed to be complete. χ may be calculated using PCFC only if a combustion temperature of isoconversion is known (i.e. the temperature in combustor for which heat of combustion in PCFC is equal to EHC in cone calorimeter). But the data are too scarce to establish a priori this temperature of isoconversion. Then, in this study, χ was calculated using PCFC and cone calorimeter and is assumed to be similar in LOI.

From Eqs. (3) and (4), it comes:

$$LOI = 21 \times \left(\frac{\beta}{\frac{HRC \times \chi \times \theta_{LOI}}{(T_{max} - T_0)}} \right)^{\frac{1}{4}} \tag{7}$$

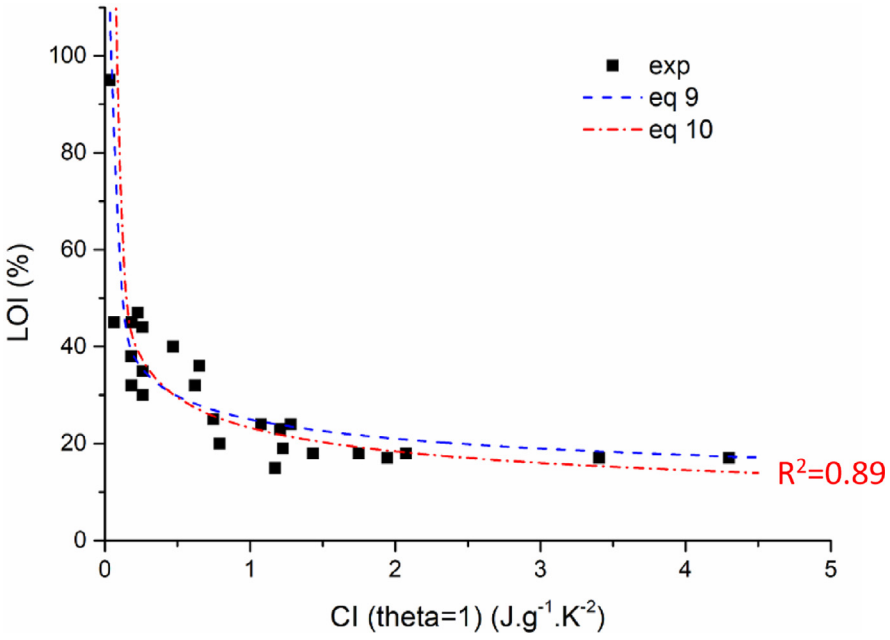


Fig. 1. LOI versus calculated index: experimental data and Eqs. (9) and (10).

The coefficient β includes all parameters supposed to be constant whatever the materials (V_{fc}, δ_f, e, α) but also the thermophysical properties (ρ, C_p) because they were shown to have minor influence on LOI.

The method proposed in this study assumes that LOI can be predicted by a so-called Calculated Index (CI) identified in Eq. (7) and mainly based on flammability parameters measured in PCFC as shown in equation 8.

$$CI = \frac{HRC * \chi * \theta_{LOI}}{(T_{max} - T_0)} \tag{8}$$

To check the validity of Eq. (7) relating LOI and CI, a set of 26 pure polymers (see Table S1 in supporting information) from [28] was used assuming that $\theta = 1$ since no flame retardant effect in condensed phase was expected. This reference provides the LOI values as well as the heat release capacity, the temperature of ignition that will be assimilated to the temperature at maximum HRR in PCFC and the combustion efficiency. Note that this assumption ($\theta = 1$) appears reasonable for most of polymers. In case of charring polymers, this assumption may be more questionable.

The experimental data were fitted using Eq. (7). The higher coefficient of determination ($R^2 = 0.88$) was obtained with $\beta = 2$, meaning that

$$LOI = 25 \times (CI)^{-\frac{1}{4}} \tag{9}$$

The data were also fitted using a power law letting free the exponent. The highest coefficient of determination ($R^2 = 0{,}89$) was obtained for the following relation:

$$LOI = 22.784 \times (CI)^{-0.341} \tag{10}$$

Since the exponent in Eq. (10) was close to that in Eq. (9) deduced from the physical theory, it was chosen to keep Eq. (10) that gives the highest coefficient of determination. Fig. 1 highlights that Eq. (10) with the new calculated index CI enables to obtain a good prediction of the LOI for pure polymers considering $\theta = 1$.

As mentioned before, considering thermophysical properties in the denominator of CI:

$CI\ therm = \frac{HRC*\chi*\theta_{LOI}}{(T_{max}-T_0)*(\rho\ *\ cp)}$ did not improve the prediction of LOI ($R^2 = 0.86$), while HRC, χ and ΔT have to be taken into account to maximize the correlation between experimental LOI and CI (with $\theta = 1$). It can be noticed that if HRC is not used in CI the correlation collapses to $R^2 = 0.65$ whereas without χ or ΔT, R^2 decreases moderately respectively to 0.83 and 0.84. This can be explained by a larger variation range of HRC or combustion efficiency compared to that of thermophysical properties.

Then for flame retardant polymers (i.e. when θ_{LOI} is not a priori equal to 1), θ_{LOI} can be extracted as follows by replacing CI in Eq. (11):

$$\theta_{LOI} = \frac{\Delta T}{HRC \times \chi} \times \left(\frac{LOI}{22.784}\right)^{-\frac{1}{0.341}} \tag{11}$$

According to Lyon et al. [17], peak of HRR measured at cone calorimeter can be related to the heat release capacity measured with PCFC by the following equations:

$$pHRR = \frac{HRC \times q''_{ext}}{n_g} \tag{12}$$

with

$$n_g = \frac{\frac{h_g}{\Delta T_p}}{X \times \theta_{CC}} \tag{13}$$

θ_{CC} can be extracted from Eqs. (12) and (13):

$$\theta_{CC} = \frac{pHRR \times h_g \times q''_{ext}}{HRC \times \Delta T_p \times X} \tag{14}$$

q''_{ext} is the external heat flux, h_g is the enthalpy of gasification with an average value considered to be 2 kJ/g and ΔT_p is the pyrolysis temperature interval (measured as the half width of HRR peak and considered equal to 50 K for pure polymers). Hence, assuming that $\theta = 1$ for pure polymers (see table S2 in supporting information), Fig. 2 shows experimental pHRR versus pHRR calculated from Eq. (12). Considering that the coefficient of correlation is acceptable ($R^2 = 0.84$), this equation can be used to extract θ_{CC} which quantifies the condensed phase efficiency in the cone calorimeter test.

In the following, these methods will be applied to flame retardant polymers in order to determine the value of θ in the case it would be different from 1. Hence condensed phase actions can be quantified and possible synergism between FR can be highlighted. For that purpose, the fire behaviour of several formulations was investigated.

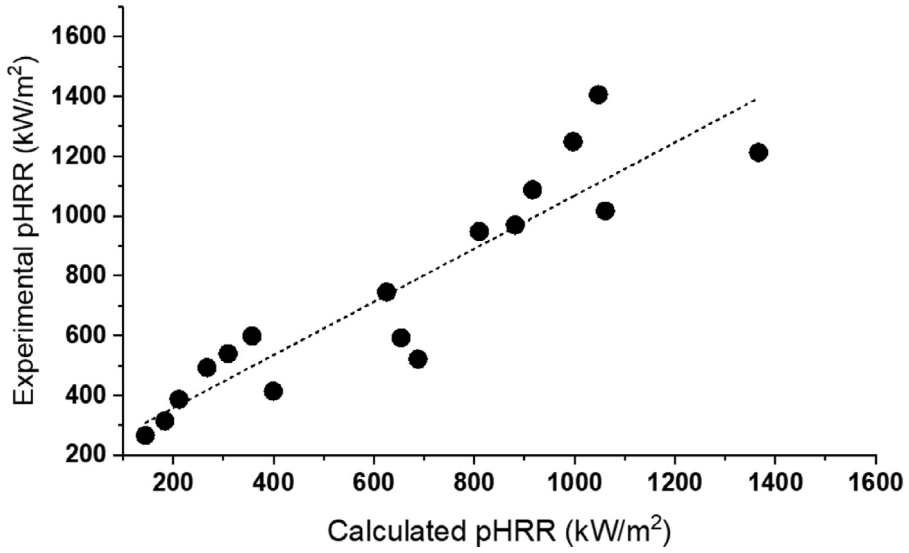


Fig. 2. Relationships between experimental pHRR measured at 50 kW/m² versus calculated pHRR.

Table 1
Detailed mass composition of the compounds studied (in wt%).

	1	2	3	4	5	6	7	8	9	10	11	12	13	14	15	16
polymers																
EVA/PE	80	60	40	80	60	40	60	40								
ABS									80	70	60	80	70	60	70	60
FR																
ATH	20	40	60				20	30								
MDH				20	40	60	20	30								
APP									20	30	40				15	20
DBDPO												20	30	40	15	20

2.2. Materials and methods

Polymers used in this study were a mixture of ethylene vinyl acetate with 26wt% of vinyl acetate (EVA Escorene UL00226CC from Exxon Mobil Chemicals) and polyethylene (LDPE PE-019 from Repsol), and acrylonitrile butadiene styrene (ABS Terluran GP22 natural from Ineos). The FRs used were Magnesium hydroxide (MDH – FR20 from ICL-IP), Aluminium hydroxide (ATH - Martinal OL104 from Huber-Martinswerk), Ammonium polyphosphate (APP Exolit AP422 from Clariant) and Decabromodiphenyloxide (DBDPO FR1210 from ICL-IP).

Compounds were extruded using a Clextral BC21 twin-screw extruder (length 90 mm, speed 200 rpm). The obtained pellets were injection moulded (Krauss Maffei 180-CX 50 t) to prepare square specimens (100 × 100 × 4 mm³). The formulations carried out for this study are detailed in the Table 1.

Each formulation was characterized using three methods. The cone calorimeter experiments were carried out using a Fire Testing Technology (FTT) apparatus. A horizontal sample sheet of 100 × 100 × 4 mm³ was placed at 25 mm below a conical heater. Samples were tested at a heat flux of 50 kW/m² with piloted ignition. All samples were tested twice. The PCFC analyses were performed with a FTT apparatus. The samples were heated from 150 to 900 °C at 1 °C/s in a pyrolyzer under nitrogen flow. Gases produced during pyrolysis were sent into a combustor and burnt at a temperature of 900 °C in presence of 20% of oxygen. In both methods, heat release rate was calculated according to the consumption of oxygen thanks to the Huggett's relation which considers that 1 kg of consumed oxygen during the combustion corresponds to 13.1 MJ of released energy. LOI was measured according to ISO 4589 specifications with a precision of 1% imposed by the accuracy of the machine using a Stanton Redcroft instrument. Tests were performed on 100 × 10 × 4 mm³ samples that were cut from the injected sheets.

3. Results and discussion

3.1. Fire performances of fr systems

3.1.1. Cone calorimeter

Some HRR curves in cone calorimeter are shown in Fig. 3. As expected, pHRR is clearly reduced when the content of fillers in the polymer increases. Particularly, in EVA/PE, the incorporation of metallic hydroxides allows increasing time-to-ignition due to the release of water through endothermic decomposition, which cools the surface of the polymer and dilutes the fuel in gas phase [29]. Moreover, MDH seems to be better than ATH to increase time-to ignition, at 60wt% TTI = 133 s for MDH and 98 s for ATH. This phenomenon is maybe due to the release of water, which occurs at low temperature for ATH when the pyrolysis has not started yet. MDH releases water at higher temperature during the first step of degradation of EVA (i.e. release of acetic acid). Percentage of ATH and MDH must be at least 60wt% in order to reach an important improvement in terms of pHRR which becomes lower than 200 kW/m². Nevertheless, it may be noticed that at 60wt% the protective layer formed by dehydrated ATH is effective longer than that formed by dehydrated MDH. This may be related to the thickness of the mineral layer. Indeed, residue from alumina (after ATH decomposition) is around 4mm-thick, while magnesium oxide forms a very thin layer. Combining the two fillers allows to combine the effects: indeed, the presence of 30wt% MDH leads to a

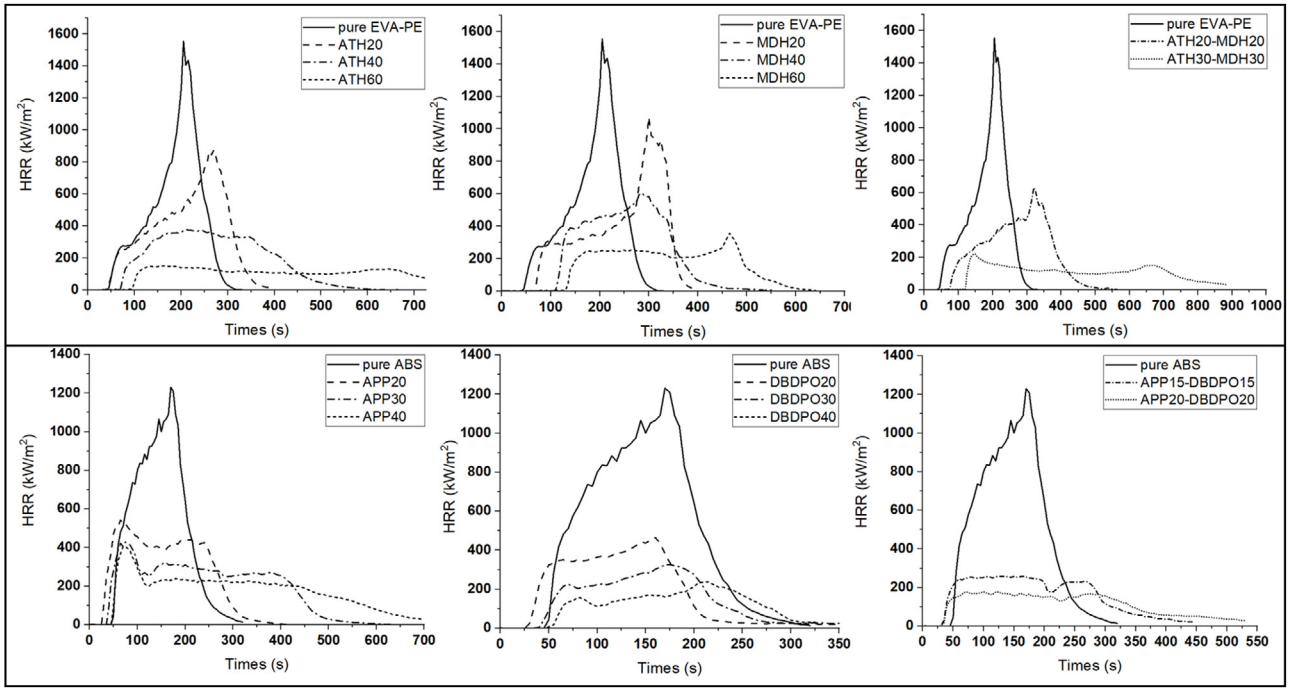


Fig. 3. Cone calorimeter curves for flame retarded EVA/PE and ABS at 50 kW/m^2.

high TTI of 120 s while the presence of 30wt% of ATH is enough to reach a significant decrease of HRR and a flaming period higher than 700 s. The second peak at 700 s may be caused by cracking char or when the pyrolysis front reaches the bottom of the sample.

Concerning flame retarded ABS compounds, using APP or DBDPO at 20wt% and 30wt% content decreases TTI. ABS containing 30wt% and 40wt% of APP shows a curve typical of a material exhibiting a barrier effect with an increase in HRR until an efficient char layer is formed and then a progressive decrease of HRR up to the flame-out.

On the contrary, DBDPO-containing ABS curves are characteristic for a non-charring material with no residue and an increase up to a quasi-static HRR that goes ahead until the pHRR occurs just before the flame out. DBDPO seems to act more efficiently than APP. The combination of the two FRs (20/20wt%) decreases the pHRR to a constant value under 200 kW/m^2 and leads to the disappearance of both the first peak of HRR observed after ignition with APP, and the second peak observed with DBDPO at the end of the test. This behaviour may indicate that DBDPO by its gas phase action hinders the peak of HRR just after ignition while APP promotes the formation of a char that leads to controlled decomposition rate up to the flame-out.

Results obtained with cone calorimeter are summarized in Figs. 4 and 5. These Figures also highlight that combining ATH and MDH do not provide a remarkable effect of synergy. From performances point of view, the combination of 20wt% APP and 20wt% DBDPO may be considered as synergistic, i.e. at the same filler content, the combination of both APP and DBDPO leads to lower pHRR than the incorporation of APP or DBDPO alone.

The thermal and thermo-oxidative decomposition of flame retarded EVA has been widely reported in the literature [30]. It takes place in two steps: the first one corresponds to a deacetylation, with the elimination of acid acetic between 300 °C and 400 °C, the second step is attributed to the degradation of unsaturated products obtained during the first step. The PCFC curves show the two pHRR corresponding respectively to the first and the second steps of the EVA decomposition.

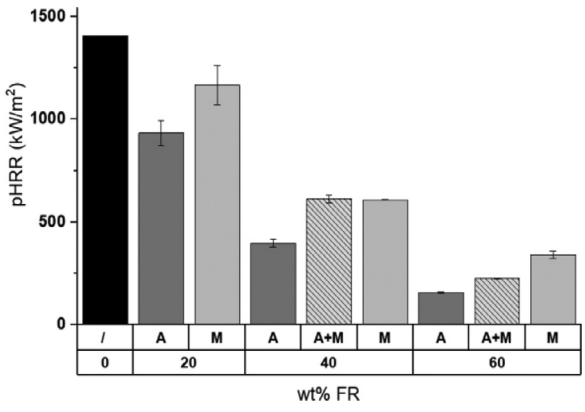


Fig. 4. pHRR in cone calorimetry (50 kW/m^2) for EVA-PE filled with ATH (A), MDH (M) and ATH+MDH (*A* + *M*).

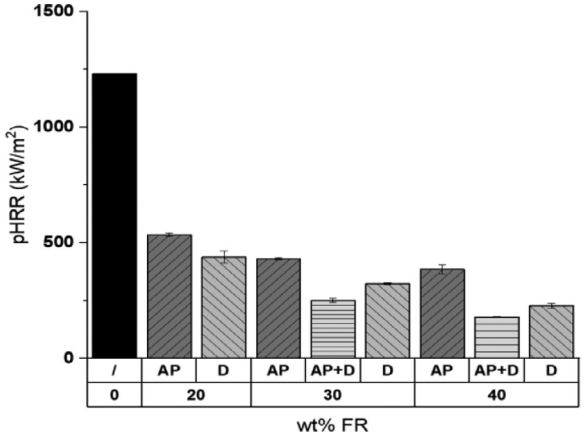


Fig. 5. pHRR in cone calorimetry (50 kW/m^2) for ABS filled with APP (AP), DBDPO (D) and APP+DBDPO (AP+*D*).

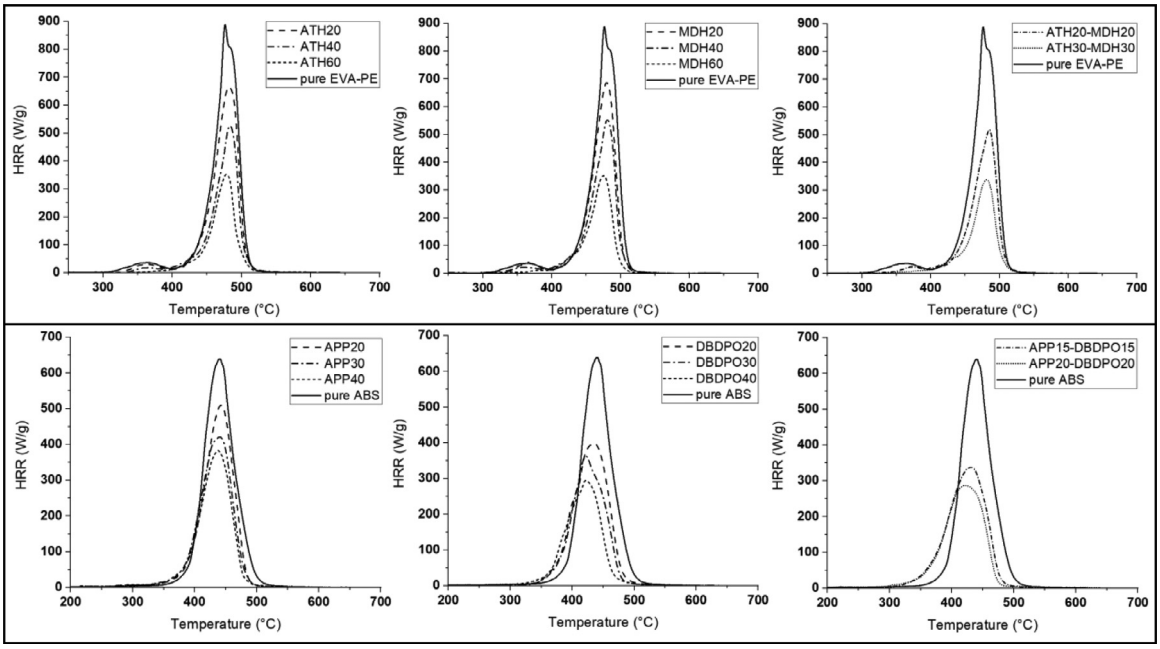


Fig. 6. PCFC curves of the flame retarded EVA/PE and ABS compounds.

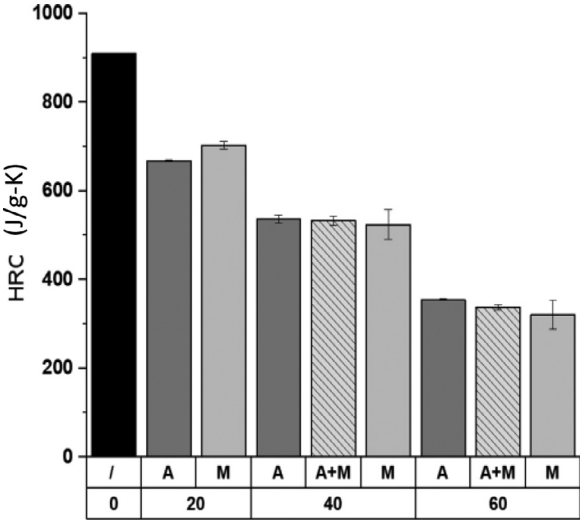


Fig. 7. HRC measured by PCFC for EVA-PE filled with ATH and MDH.

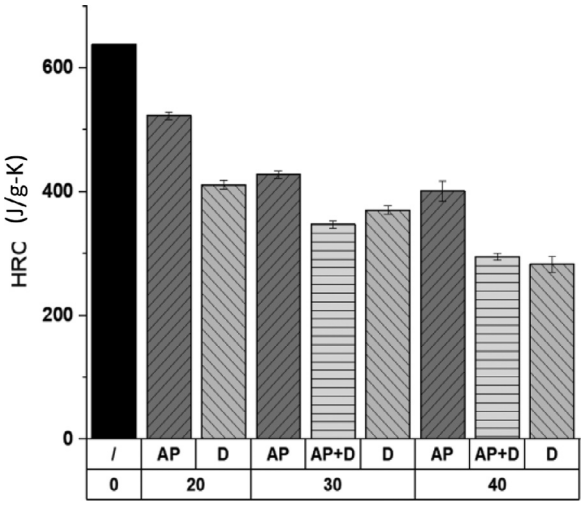


Fig. 8. HRC measured by PCFC for ABS filled with APP and DBDPO.

PCFC results show a decrease of HRR for each filler (Fig. 6). The reduction in pHRR for all compounds is less distinct than in cone calorimeter test. Moreover, for EVA/PE compounds, the decrease of HRR is proportional to the filler content: ATH and MDH act in a very similar way, with a decrease in HRC of 20%, 40% and more than 50% for respectively 20wt%, 40wt% and 60wt% of fillers, then this decrease is almost exclusively assigned to the dilution of the condensed phase. Results obtained with PCFC are summarized in Figs. 7 and 8. The mixture of ATH and MDH does not show any synergy since HRC of the blends is approximately equal to the mean value of HRCs of the components. PCFC does not consider physical effects like the barrier effect because of the sample size (2 mg). Flame inhibition (from DBDPO) is also not effective in PCFC in standard conditions. Nevertheless, for ABS compounds, the decrease of HRR is lower with APP than with DBDPO. As an example, with a 40wt% filler content, the HRC decreases by 56% with DBDPO while the decrease is only 37% with APP. Concerning the mixture of the two FRs, the decrease in HRC for 40wt%(APP+DBDPO) is close to the formulation with 40wt% of DBDPO.

In LOI, for both polymers and with the different flame-retardants, the increase of FR content leads to the increase of LOI. This effect appears exponential for ATH or MDH in EVA/PE and DBDPO in ABS. Fig. 9 shows that in EVA/PE containing ATH or MDH, LOI values are not significantly different and, once again, no effect of synergy was observed for this parameter when combining ATH and MDH. For ABS, DBDPO is much more efficient than APP. No effect of synergy was observed, i.e. the mixture of both additives does not have a greater effect than each one considered separately. On the contrary, the formulations containing both fillers have the same behaviour than those containing only APP. Hence, the fire spreads slowly and the test ended because of the time of combustion was higher than 3 min for oxygen index (OI) < LOI. On the contrary, for ABS filled with DBDPO only, the behaviour was completely different with a rapid extinction for OI < LOI and a faster flame spread for OI ≥ LOI. Then, the mode of action of

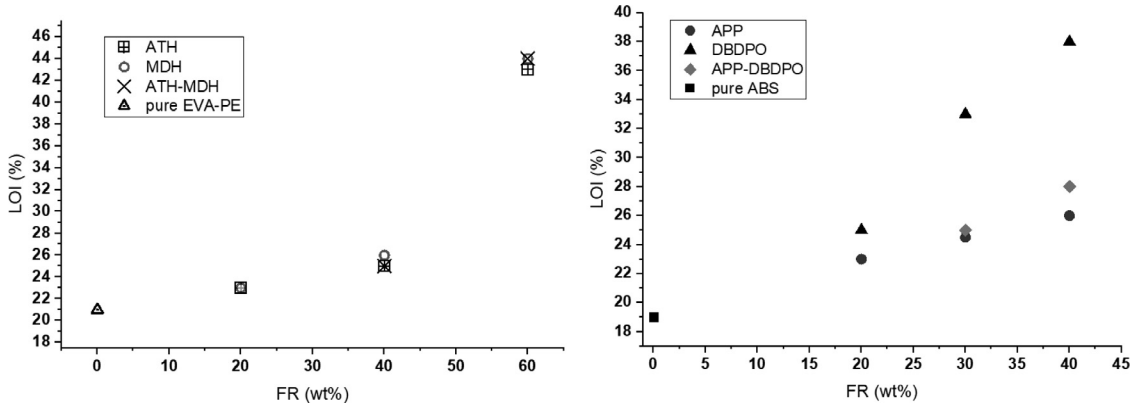


Fig. 9. LOI versus FR content for EVA-PE systems and ABS systems.

Table 2
Main results of cone calorimeter, PCFC and LOI tests.

		Cone calorimeter			PCFC				LOI
	FRwt%	pHRR (kW/m²)	EHC (kJ/g)	χ	HRC (J/g.K)	HCC (kJ/g)	ΔT(°C)	ΔT_p(°C)	LOI (%)
EVA/PE	0%	1407	35.8	0.92	910	38.9	452	38.5	21
ATH	20%	934	33.2	0.98	668	33.9	457	37.3	23
	40%	397	29.4	0.93	537	31.8	457	34.4	25
	60%	156	23.5	0.93	355	25.1	454	32.4	43
MDH	20%	1166	33.8	0.95	703	35.6	456	36.6	23
	40%	608	31.0	0.94	524	33.0	456	35.6	26
	60%	340	25.7	0.98	321	26.4	450	39.2	44
ATH-MDH	40%	613	30.3	0.95	533	31.9	460	35.5	25
	60%	225	25.0	0.97	338	25.7	455	34.4	44
ABS	0%	1231	30.0	0.86	638	34.8	414	53.2	19
APP	20%	535	25.0	0.73	523	34.4	415	58.1	23
	30%	432	28.5	0.98	428	29.1	413	56.2	24.5
	40%	385	30.7	1.12	401	27.4	411	56.4	26
DBDPO	20%	438	11.7	0.40	411	29.3	404	63	25
	30%	323	8.6	0.35	370	24.8	394	61.3	33
	40%	227	7.0	0.34	284	20.8	394	68.1	38
APP-DBDPO	30%	251	14.1	0.46	347	30.3	397	69.4	25
	40%	179	11.4	0.39	295	29.3	397	70.8	28

APP seems to limit the flame inhibition of DBDPO in LOI test. In our case, it seems that mixing a brominated FR, which acts in gas phase by flame inhibition, and APP that acts in condensed phase as char promoter leads to an antagonistic effect in LOI test.

All main data from cone calorimeter, PCFC and LOI tests are summarized in Table 2. The combustion efficiency χ is close to one for the majority of the formulations, except for DBDPO compounds with a combustion efficiency around 0.40, even in presence of APP. This low value illustrates the flame inhibition of this halogenated flame retardant.

Horrocks et al. [31] applied a linear methodology in order to define a synergistic effect, using the following equation:

$$SE = \frac{(OI_{FR+S+P} - OI_P)}{((OI_{FR+P} - OI_P) + (OI_{S+P} - OI_P))} \quad (15)$$

Where OI_{FR+P+S} is the OI for polymer containing a flame retardant with a synergist. In our case, for the formulations containing two flame retardants, one of the additives is considered as the synergist. Thus Eq. (15) can be applied in order to evaluate the potential synergistic effect between ATH and MDH in EVA/PE and between APP and DBDPO in ABS. In the case of EVA/PE filled with 60wt% of ATH and MDH, SE was equal to 2.6, supposing a good synergy between ATH and MDH, while SE was only 1 for 40wt% of ATH and MDH. This confirms the need to use high filler content in order to optimize the FR efficiency. Nevertheless, previously we showed that 60wt% of ATH or MDH have the same impact than 60wt% of [ATH+MDH]. Then the index proposed by Horrocks is not representative in our case. For flame retarded ABS with 40wt% of APP and DBDPO, SE was equal to 0.9 illustrating an antagonistic effect, as actually observed.

Contrary to LOI, some synergistic effects can be observed in other tests. The most obvious synergy is observed between APP and DBDPO in ABS in the cone calorimeter test since pHRR of the formulations containing the additive mixture is lower than that of compositions containing only one filler at the same total content. Since this synergy was not noticeable in the LOI measurements, it can be concluded that synergies depend on the test used. Note that synergism is only considered from a performance point of view, i.e. without considering the supposed underlying mechanism.

3.1.2. Assessment of FR efficiency in condensed phase

Assuming that LOI and pHRR in cone calorimeter of flame-retardant polymers can be predicted according to Eqs. (11) and (14), θ was determined for the EVA/PE and ABS flame retarded formulations. Although the Eqs. (10) and (12) allow assessing LOI and pHRR with an acceptable accuracy for pure polymers, θ is not strictly equal to 1. In order to compare the efficiency of different FR systems in a same polymer (ABS or EVA/PE), reduced values of relative efficiency of heat and mass transfer at the surface $\theta_{LOI\ r}$ or $\theta_{cc\ r}$ are introduced.

$$\theta_r = \frac{\theta_{\ FR\ \ polymer}}{\theta_{\ pure\ \ polymer}} \quad (16)$$

θ values are summarized in Table 3. Uncertainties of θ were evaluated using the variance formula, Eq. (17), and considering

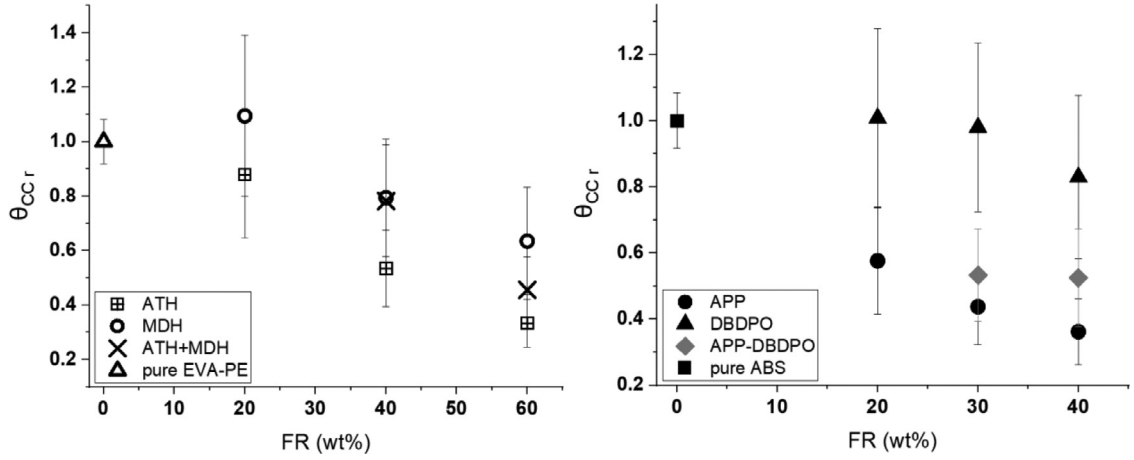


Fig. 10. $\theta_{CC\ r}$ versus FR content for EVA-PE compounds and ABS compounds.

Table 3
θ and $\theta_{\ r}$ for the formulations studied.

	Wt% FR	θ_{LOI}	$\theta_{LOI\ r}$	θ_{CC}	$\theta_{\ CC\ r}$
EVA/PE	/	0.74	**1**± 0.06	1.74	**1** ± 0.08
ATH	20	0.74	**1.00** ± 0.06	1.53	**0.88** ± 0.23
	40	0.76	**1.04** ± 0.1	0.93	**0.53** ± 0.14
	60	0.24	**0.33** ± 0.03	0.58	**0.33** ± 0.09
MDH	20	0.72	**0.98** ± 0.08	1.91	**1.09** ± 0.3
	40	0.69	**0.93** ± 0.13	1.38	**0.79** ± 0.22
	60	0.24	**0.32** ± 0.06	1.11	**0.64** ± 0.2
ATH-MDH	40	0.75	**1.02** ± 0.09	1.36	**0.78** ± 0.2
	60	0.23	**0.31** ± 0.03	0.79	**0.46** ± 0.12
ABS	/	1.37	**1** ± 0.07	1.79	**1** ± 0.08
APP	20	1.50	**1.09** ± 0.09	1.34	**0.58** ± 0.16
	30	0.87	**0.63** ± 0.04	1.13	**0.44** ± 0.11
	40	0.68	**0.50** ± 0.04	0.83	**0.36** ± 0.1
DBDPO	20	1.33	**0.97** ± 0.05	2.14	**1.01** ± 0.27
	30	1.15	**0.84** ± 0.05	2.02	**0.98** ± 0.26
	40	1.03	**0.75** ± 0.08	1.90	**0.83** ± 0.25
APP-DBDPO	30	2.05	**1.49** ± 0.09	1.24	**0.53** ± 0.14
	40	2.08	**1.52** ± 0.15	1.25	**0.52** ± 0.15

the standard deviation of each parameter. Typically, standard deviations are ± 15 J/g.K, ± 2 K, ± 0.03, ± 500 J/g, ± 1% and ± 20 kW/m^2, respectively for the parameters HRC, ΔT and ΔT_p, χ, h_g LOI and pHRR.

$$u_c^2(y) = \sum_{i=1}^{n} \left(\frac{df}{dxi} \right)^2 u^2(xi) \tag{17}$$

With u(x_i) the standard deviation of the parameter x_i. The uncertainty of $\theta_{\ CC\ r}$ is much more important than that of $\theta_{LOI\ r}$ due to the high standard deviation of the enthalpy of gasification (2000 ± 500 J/g according to Lyon et al. [17]).

3.1.3. Assessment of FR efficiency in condensed phase in cone calorimeter

Fig. 10 reports θ_{CC} values for the flame-retarded compounds. It is noteworthy that, despite some large standard deviations, the discrepancy between formulations is much important, therefore conclusions can be drawn.

In EVA/PE blends, no effect in gas phase was observed for ATH or MDH according to combustion efficiency values (close to 1 in all cases). ATH exhibits a higher condensed phase efficiency compared to MDH in EVA/PE compounds. This result is related to the thickness of the mineral residue and is in agreement with the HRR curve shape in cone calorimeter. According to [32], the curve shape is representative of an efficient barrier effect in the case of ATH-based formulations (at 60wt% of FR). Additionally, the results confirm that there is no synergism between ATH and MDH.

$\theta_{CC\ r}$ for ABS formulations containing APP decreases (about 0.6 at 40wt% content). This result evidence the charring promotion by the phosphorus FR. On the contrary, $\theta_{CC\ r}$ is close to 1 for DBDPO-based formulations, highlighting that FR acts only in gas phase and does not promote any charring. The smaller is $\theta_{CC\ r}$, the better is the efficiency in condensed phase.

Table 4 shows the residue content r obtained in PCFC and cone calorimeter. On the whole, for EVA/PE formulations, residues are roughly the same in both tests. It may be noticed that the fraction of residue is correlated with θ. This confirms the condensed phase mode of action of those fillers even if not only the char content but also its structure has an effect on its insulating character as barrier layer. For ABS, the residue of APP containing formulations is significantly higher in cone calorimeter test: it means that barrier effect in cone calorimeter leads to incomplete pyrolysis (residue contains not only char but also a fraction of unpyrolyzed polymer). On the contrary, formulations with DPDPO are almost totally consumed whatever the test.

3.1.4. Assessment of FR efficiency in condensed phase in LOI

The influence of each FR system was assessed for all the flame retarded polymers using the calculated index. The values of θ for the LOI test can be deduced from Eq. (16) using all the parameters collected at the previous tests. The values are listed in Table 2.

In EVA/PE compounds, $\theta_{LOI\ r}$ decreases from 1 to 0.33 and 0.32 for 60wt% of ATH and MDH respectively. However, with only 20wt% and 40wt% of fillers, $\theta_{LOI\ r}$ does not decrease. At these filler contents, LOI increases moderately from 21% to 25% (40wt% ATH) and 26% (40wt%MDH), that is mainly due to the decrease in HRC, resulting from the dilution of the condensed phase (i.e. the polymer is partly replaced by the mineral fillers). It is well known that ATH and MDH need to be used at a content equal or greater than 60wt% to be efficient, below this content, the mode of action in condensed phase is not significant in LOI. For the ABS-based formulations containing APP, $\theta_{LOI\ r}$ decreases from 1 to 0.50 with 40wt% fillers. By comparison, DBDPO induces a limited decrease of θ_r from 1 to 0.75 while LOI increases more than with APP. As expected, this shows that APP, as a phosphorus flame retardant, has an important condensed phase effect with the formation of a char. On the contrary, DBDPO mainly acts in the vapour phase and traps radicals propagating thermal oxidation in the flame. That is why θ_r remains higher for DBDPO compounds while χ is assumed to be significantly reduced (according to cone calorimeter data) (Fig. 11).

Table 4
Experimental percentage of residue for flame retarded EVA/PE and ABS in cone calorimeter and PCFC.

	EVA/PE	ATH			MDH			ATH-MDH		ABS	APP			DBDPO			APP-DBDPO	
Wt%	100%	20%	40%	60%	20%	40%	60%	40%	60%	0%	20%	30%	40%	20%	30%	40%	30%	40%
r_{CC} (%)	0	14	26	42	16	28	43	28	42	0	14	24	30	0.4	4	7	16	20
r_{PCFC} (%)	0	11	26	39	13	28	41	25	40	0	11.8	8.3	17.4	4.7	4	2.7	13	20.6

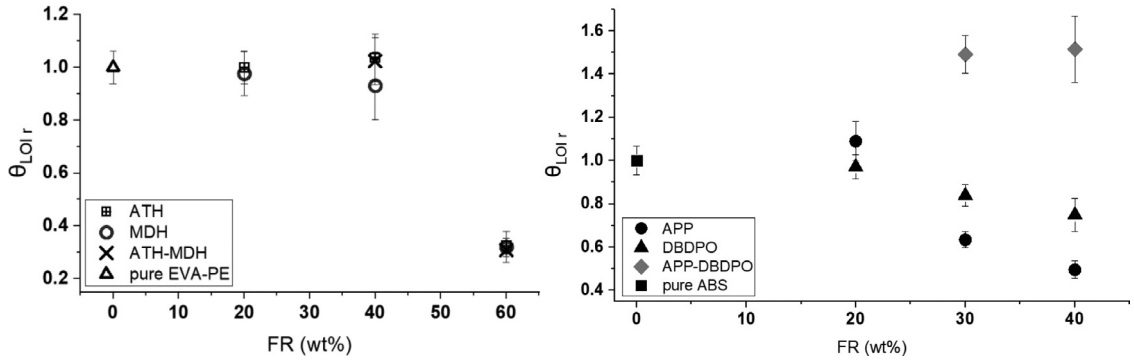


Fig. 11. $\theta_{LOI\ r}$ versus FR content for EVA-PE compounds and ABS compounds.

Furthermore, APP and DBDPO lead to a strong antagonistic effect in condensed phase since Fig. 11 shows an increase of θ to values largely higher than 1. The combustion efficiency remaining low for the APP/DBDPO combination (χ between 0.39 and 0.46 in cone calorimeter), the low values of LOI would not be related to an inefficient action of DBDPO in gas phase. It may be noticed that this result depends on the assumption that χ which was calculated using PCFC and cone calorimeter is similar in LOI. Further investigation is needed to check this assumption.

3.1.5. Respective contribution of combustion efficiency and phase condensed efficiency

Since DBDPO and APP act through different modes-of-action, the discussion is focused on the ABS formulations in cone calorimeter. The gas phase effect of DBDPO inhibits the combustion whereas the charring promotion from APP traps the fuel in the solid by charring and/or promotes barrier effect through the formation of protective residue layer.

In flame retarded ABS compounds, both modes of action can be active. Fig. 12 plots $\theta_{CC\ r}$ versus χ for ABS formulations. The first diagonal represents the situation where the combustion efficiency is equal to the condensed phase efficiency. Thus, the contribution of the combustion efficiency and the condensed phase efficiency is revealed using such a graph. Hence, for ABS/APP-DBDPO [70/30], the decrease in $\theta_{CC\ r}$ is 37% while the decrease in χ is 46%. Thus, the respective contribution of condensed phase efficiency can be evaluated to be 37/(37+46)x100 = 45% and the part of combustion efficiency is equal to 46/(37+46)x100 = 55% .

The decrease in $\theta_{CC\ r}$ corresponds to the condensed phase effect whereas the decrease in χ corresponds to the combustion efficiency illustrating the gas phase mode of action. Hence, "isoefficiency" curves for which $\chi\theta$ = constant can be plotted. $\chi\theta$ is considered as the burning efficiency and isoefficiency curves allow to illustrate the graphical position of all mixtures with the same efficiency. Thus, it appears that ABS filled with 20wt% APP and 20wt% DBDPO has a burning efficiency of 0.25.

For this latter composition, a synergy (i.e. a lower pHRR than corresponding formulations with the same content of only one FR) was highlighted in cone calorimeter. Isoefficiency curves reveal that the burning efficiency is actually lower for the formulations containing both FRs.

However, the term "synergy" is debatable. Indeed, Fig. 13 shows the evolution of $\theta_{CC\ r}$ and χ in ABS as function of respectively APP and DBDPO content. This clearly reveals that θ and χ do not decrease linearly with the FR content. In both cases, there is a strong decrease at low filler content and then the FR efficiency seems to reach a plateau from 20wt% for DBDPO and from 30wt% for APP. In these conditions, the rule of mixtures is probably not appropriate to evidence a synergy effect. Obviously, the efficiency of 20wt% DBDPO in ABS/DBDPO/APP (60/20/20) will be higher than half of the efficiency of 40wt% DBDPO in ABS/DBDPO (60/40) without considering any interaction between DBDPO and APP.

Considering Fig. 13 and assuming an additive contribution of gas phase and condensed phase effects, it can be supposed that the best burning efficiency at the lowest filler content is reached for DBDPO/ABS ratio of 20/80 and APP/ABS ratio of 30/70. Solving this equation system would lead to an optimal ABS/DBDPO/APP composition with the ratio 60/15/25.

$\theta_{CC\ r}$ for ABS with 20wt% APP and χ for ABS with 20wt% DBDPO are equal to 0.58 and 0.40 respectively. The product is equal to 0.23, i.e. very close to the burning efficiency obtained for the formulation containing 20wt% of APP and 20wt% of DBDPO (0.25) which exhibits values of 0.52 and 0.39 for $\theta_{CC\ r}$ and χ respectively. Based on such analysis, the combination APP/DBDPO seems to act according to a simple additive effect without interactions between both fillers. This analysis illustrates that the synergy is not so obvious between the two additives. This is particularly due to the fact that their separate effect does not vary linearly with their content as shown in Fig. 13.

4. Conclusion

In this study, the efficiency of different FR systems in condensed phase was assessed using equations predicting the LOI and pHRR from a couple of parameters. The equation for pHRR in cone calorimeter has been proposed by Lyon while the equation for LOI was obtained from a set of 26 pure polymers. In both cases, the reliability of these equations was checked assuming that the efficiency in condensed phase is equal to 1 for pure polymers.

The values for the efficiency in condensed phase are in agreement with the expected modes-of-action of the FR systems stud-

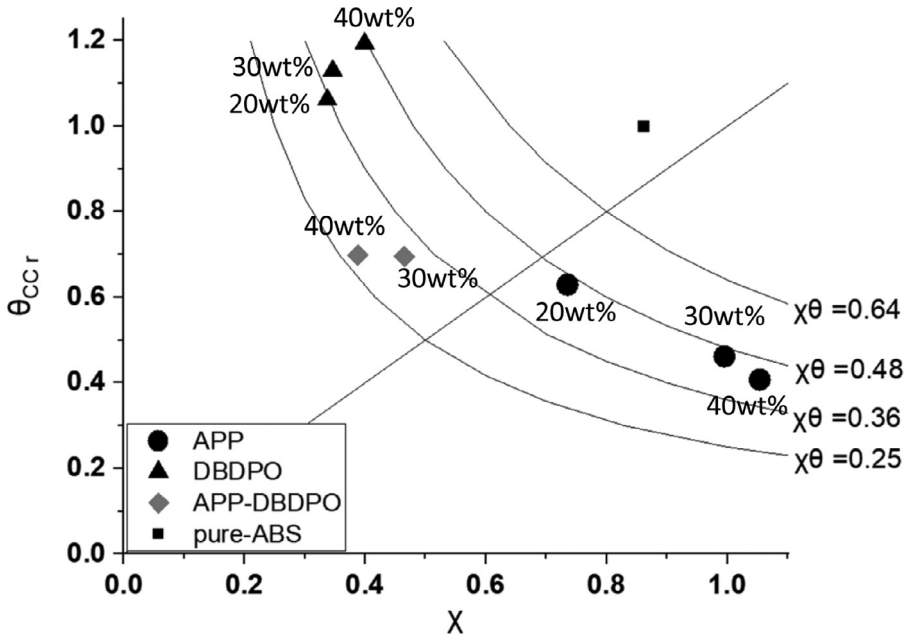


Fig. 12. θ_{CC} r versus χ for flame retarded ABS compounds and several isoefficiency curves.

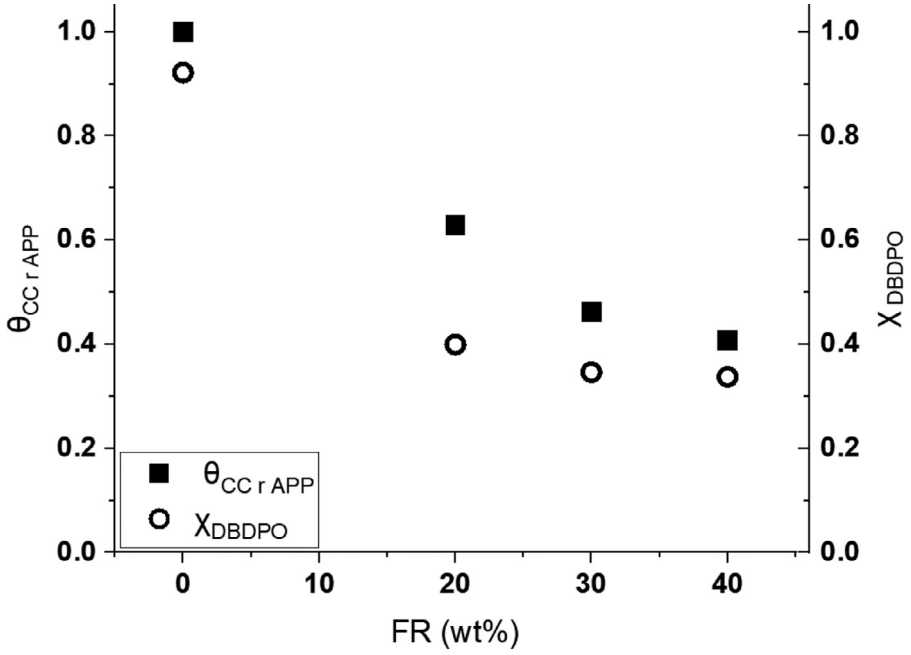


Fig. 13. Evolution of $\theta_{CC\ r}$ and χ according to the content of APP and DBDPO respectively.

ied. ATH and MDH act in condensed phase but their action is efficient only for high contents (40wt% in cone calorimeter and 60wt% in LOI). APP acts only in condensed phase (low θ and χ close to 1) while DBDPO is an efficient flame inhibitor acting manly in gas phase (θ close to 1 and low χ).

The method allows a quantitative assessment of the modes-of-action by discriminating actions in gas and condensed phases. Isoefficiency curves can be drawn to identify the modes-of-action, from pure flame inhibitor (θ close to 1 and low χ) to char promoter (χ close to 1 and low θ).

It also provides information about synergistic or antagonistic effect. Combining ATH and MDH does not seem to be a suitable strategy. On the contrary, strong negative or positive interactions have been highlighted between APP and DBDPO. Antagonism was pointed out in LOI, through a high θ value (considering that χ is the same in LOI and in cone calorimeter).

Nevertheless, synergism may be falsely postulated because the effect of a flame retardant is not proportional to its content. Indeed, synergism was apparently highlighted in the cone calorimeter test from a performance point of view. The combination APP/DBDPO (20/20) shows a low χ (i.e. a high efficiency in gas phase) and an intermediate θ (between the values for DBDPO and APP only). Nevertheless, the efficiency burning is similar to the product of θ for ABS filled with 20wt% APP and χ for ABS filled with 20wt% DBDPO (i.e. considering that both FR act independently, one in condensed phase and the second in gas phase exclusively). Therefore, synergism between APP and DBDPO is questionable.

Declaration of Competing Interest

The authors declare that they have no known competing financial interests or personal relationships that could have appeared to influence the work reported in this paper.

Supplementary materials

Supplementary material associated with this article can be found, in the online version, at doi:10.1016/j.polymdegradstab.2021.109767.

CRediT authorship contribution statement

Mathieu Vangrevelynghe: Conceptualization, Formal analysis, Investigation, Methodology, Validation, Writing – original draft. **Lucie Le Nouvel:** Formal analysis, Investigation. **Cécile Pesenti:** Formal analysis, Investigation. **Rodolphe Sonnier:** Conceptualization, Methodology, Supervision, Validation, Writing – review & editing. **Laurent Ferry:** Conceptualization, Methodology, Supervision, Validation, Writing – review & editing. **Emmanuelle Gesta:** Funding acquisition, Supervision, Writing – review & editing. **Christian Lagrève:** Funding acquisition, Supervision, Writing – review & editing.

References

[1] F. Laoutid, L. Bonnaud, M. Alexandre, J.M. Lopez-Cuesta, P. Dubois, New prospects in flame retardant polymer materials: from fundamentals to nanocomposites, Mater. Sci. Eng. R Reports 63 (2009) 100–125.

[2] T.R. Hull, A. Witkowski, L. Hollingbery, Fire retardant action of mineral fillers, Polym. Degrad. Stab. 96 (2011) 1462–1469.

[3] R.N. Rothon, P.R. Hornsby, Flame retardant effects of magnesium hydroxide, Polym. Degrad. Stab. 54 (1996) 383–385.

[4] F. Laoutid, L. Ferry, E. Leroy, J.M. Lopez Cuesta, Intumescent mineral fire retardant systems in ethylene-vinyl acetate copolymer: effect of silica particles on char cohesion, Polym. Degrad. Stab. 91 (2006) 2140–2145.

[5] G. Beyer, Flame retardant properties of EVA-nanocomposites and improvements by combination of nanofillers with aluminium trihydrate, Fire Mater 25 (2001) 193–197.

[6] M.A. Cárdenas, D. García-López, I. Gobernado-Mitre, J.C. Merino, J.M. Pastor, J. Martínez, D. de, J. Barbeta, D. Calveras, Mechanical and fire retardant properties of EVA/clay/ATH nanocomposites - Effect of particle size and surface treatment of ATH filler, Polym. Degrad. Stab. 93 (2008) 2032–2037.

[7] L. Wang, X. He, C.A. Wilkie, The utility of nanocomposites in fire retardancy, Materials (Basel) 3 (2010) 4580–4606.

[8] J. Lv, W. Liu, Flame retardancy and mechanical properties of EVA nanocomposites based on magnesium hydroxide nanoparticles/microcapsulated red phosphorus, J. Appl. Polym. Sci. 105 (2007) 333–340.

[9] Khanna, Y.P.; Pearce, E.M. Flame - Retardant Polymeric Materials; Lewin, M., Atlas, S.M., Pearce, E.M., Eds.; Springer US: Boston, MA, 1978; ISBN 978-1-4684-6975-2.

[10] S. Bourbigot, J. Sarazin, F. Samyn, M. Jimenez, Intumescent ethylene-vinyl acetate copolymer: reaction to fire and mechanistic aspects, Polym. Degrad. Stab. 161 (2019) 235–244.

[11] S. Bourbigot, M. Le Bras, S. Duquesne, M. Rochery, Recent Advances for Intumescent Polymers, Macromol. Mater. Eng. 289 (2004) 499–511.

[12] J.M. Cogen, T.S. Lin, R.E. Lyon, Correlations between pyrolysis combustion flow calorimetry and conventional flammability tests with halogen-free flame retardant polyolefin compounds, Fire Mater 33 (2009) 33–50.

[13] B. Schartel, K.H. Pawlowski, R.E. Lyon, Pyrolysis combustion flow calorimeter: a tool to assess flame retarded PC/ABS materials? Thermochim. Acta 462 (2007) 1–14.

[14] R. Sonnier, L. Ferry, C. Longuet, F. Laoutid, B. Friederich, A. Laachachi, J.-.M. Lopez-Cuesta, Combining cone calorimeter and PCFC to determine the mode of action of flame-retardant additives, Polym. Adv. Technol. 22 (2011) 1091–1099.

[15] R. Sonnier, H. Vahabi, L. Ferry, J.-.M. Lopez-Cuesta, Pyrolysis-Combustion Flow Calorimetry: a Powerful Tool To Evaluate the Flame Retardancy of Polymers, ACS Symposium Series 1118 (2012) 361–390 ISBN 9780841227804.

[16] Van Krevelen, D.W. Some basic aspects of flame resistance of polymeric materials. 1975, 16, 615–620.

[17] R.E. Lyon, R.N. Walters, S.I. Stoliarov, Screening flame retardants for plastics using microscale combustion calorimetry, Polym. Eng. Sci. 47 (2007) 1501–1510.

[18] R.E. Lyon, N. Safronava, S. Crowley, R.N. Walters, A molecular-level fire growth parameter, Polym. Degrad. Stab. 186 (2021) 109478.

[19] R.E. Lyon, R.N. Walters, Pyrolysis combustion flow calorimetry, J. Anal. Appl. Pyrolysis 71 (2004) 27–46.

[20] B. Schartel, C.A. Wilkie, G. Camino, Recommendations on the scientific approach to polymer flame retardancy: part 1 - Scientific terms and methods, J. Fire Sci. 34 (2016) 447–467.

[21] B. Camino, G. Camino, The chemical kinetics of the polymer combustion allows for inherent fire retardant synergism, Polym. Degrad. Stab. 160 (2019) 142–147.

[22] M. Lewin, Synergism and catalysis in flame retardancy of polymers, Polym. Adv. Technol. 12 (2001) 215–222.

[23] A.F. Holdsworth, A.R. Horrocks, B.K. Kandola, Novel metal complexes as potential synergists with phosphorus based flame retardants in polyamide 6.6, Polym. Degrad. Stab. (2020) 179.

[24] J. Quintiere, A simplified theory for generalizing results from a radiant panel rate of flame spread apparatus, Fire Mater 5 (1981) 52–60.

[25] A. Nasr, S. Suard, H. El-Rabii, L. Gay, J.-.P. Garo, Fuel Mass-Loss Rate Determination in a Confined and Mechanically Ventilated Compartment Fire Using a Global Approach, Combust. Sci. Technol. 183 (2011) 1342–1359.

[26] P.M. Hergenrother, C.M. Thompson, J.G. Smith, J.W. Connell, J.A. Hinkley, R.E. Lyon, R. Moulton, Flame retardant aircraft epoxy resins containing phosphorus, Polymer (Guildf) 46 (2005) 5012–5024.

[27] R. Sonnier, B. Otazaghine, L. Ferry, J.M. Lopez-Cuesta, Study of the combustion efficiency of polymers using a pyrolysis-combustion flow calorimeter, Combust. Flame 160 (2013) 2182–2193.

[28] R.E. Lyon, M.L. Janssens, Polymer Flammability. In Encyclopedia of Polymer Science and Technology, Wiley (2015) 1–70 ISBN 0471440264.

[29] G. Camino, A. Maffezzoli, M. Braglia, M. De Lazzaro, M. Zammarano, Effect of hydroxides and hydroxycarbonate structure on fire retardant effectiveness and mechanical properties in ethylene-vinyl acetate copolymer, Polym. Degrad. Stab. 74 (2001) 457–464.

[30] B.J. Holland, J.N. Hay, The thermal degradation of poly(vinyl acetate) measured by thermal analysis–Fourier transform infrared spectroscopy, Polymer (Guildf) 43 (2002) 2207–2211.

[31] A.R. Horrocks, G. Smart, S. Nazaré, B. Kandola, D. Price, Quantification of Zinc Hydroxystannate and Stannate Synergies in Halogen-containing Flame-retardant Polymeric Formulations, J. Fire Sci. 28 (2010) 217–248.

[32] B. Schartel, T.R. Hull, Development of fire-retarded materials—Interpretation of cone calorimeter data, Fire Mater 31 (2007) 327–354.